Paper Title: Algorithm and Implementation of High-Dynamics Pulse-Shaped Signals Simulation

Authors: Shaozhong Lu, Yongqing Wang, Sheng Li, Siliang Wu

Manuscript ID: SCIS-2016-0541

Date: Dec 28, 2016

Supplement

I. Derivation of high-dynamic pulse-shaped signal model

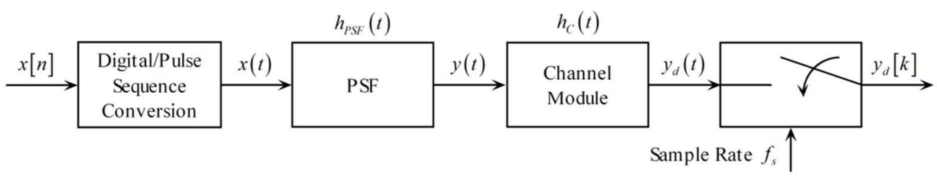

Figure 1. Hybrid analog/digital model for high-dynamics pulse-shaped signal modeling.

The modeling process for high-dynamics pulse-shaped signals can be interpreted with a hybrid analog/digital model, as depicted in Figure 1.

The continuous-time baseband data pulse sequence signal $x(t)$ obtained after digital/pulse sequence conversion can be expressed as

$$x(t)=\sum_{n=-\infty}^{\infty} x[n]\delta(t-nT_0), \tag{1}$$

where $x[n]$ is the digital data sequence and T_0 is the fixed data cycle period. The PSF filters $x(t)$ and outputs a non-dynamic pulse-shaped signal $y(t)$:

$$y(t)=\sum_{n=-\infty}^{\infty} x[n]h_{PSF}(t-nT_0). \tag{2}$$

The channel module is then used to simulate the transmission delay characteristics in the high-speed environment. Let the channel module frequency response be $H_C(j\Omega)$, which can be written as

$$H_C(j\Omega)=e^{-j\Omega D}, \tag{3}$$

where parameter D is the transmission delay. Therefore, the continuous-time high-dynamics pulse-shaped signal is obtained as

$$y_d(t)=\sum_{n=-\infty}^{\infty}x[n]h_{PSF}(t-D-nT_0). \tag{4}$$

The discrete-time high-dynamics pulse-shaped sequence resulting from sampling the continuous-time signal in (4) at time instants $t=kT_s$ ($T_s=1/f_s$ is the sample period) is given by

$$y_d[k]=\sum_{n=-\infty}^{\infty}x[n]h_{PSF}(kT_s-D-nT_0), \tag{5}$$

where $y_d[k]=y_d(kT_s)$.

According to the interpolation theory, basepoint index m_k and fractional interval μ_k are defined as

$$\begin{aligned} m_k &= \left\lfloor \frac{kT_s-D}{T_0} \right\rfloor \\ \mu_k &= \frac{kT_s-D}{T_0}-m_k \end{aligned}, \tag{6}$$

where $\lfloor x \rfloor$ is the floor operator. Equation (5) can then be rewritten as

$$y_d[k]=\sum_{i=-I}^{I-1}x[m_k-i]h_{PSF}[(i+\mu_k)T_0], \tag{7}$$

where $i=m_k-n$.

II. Derivation of parameters m_k and μ_k

Transmission delay D can be defined as

$$D=\frac{d(t)}{c}, \tag{8}$$

where c is the speed of light, and $d(t)$ is the signal propagation path length at received time t, expressed as

$$d(t)=d_0+\int_0^t v(\tau)d\tau, \tag{9}$$

where d_0 is the initial distance at $t=0$, and $v(t)$ is the receiver speed. We assume here that the transmitter is stationary. In terms of the Doppler effect, the Doppler data rate is defined as

$$R_d(t) = -\frac{v(t)}{c} R_0 , \tag{10}$$

where $R_0 = 1/T_0$ is the transmission data rate. Substituting (10) into (9) gives

$$d(t) = d_0 - \frac{c}{R_0} \int_0^t R_d(\tau) d\tau , \tag{11}$$

whose corresponding discrete expression is

$$d(kT_s) = d_0 - \frac{c}{R_0} \sum_{n=0}^{k} R_d[n] T_s . \tag{12}$$

In (12), $R_d[n] = R_d(nT_s)$ is the discrete Doppler data rate. Substituting (12) and (8) into (6) yields

$$\begin{aligned} m_k &= \left\lfloor \sum_{n=0}^{k} \left(R_0 + R_d[n]\right) T_s - \frac{d_0}{c} R_0 \right\rfloor \\ \mu_k &= \sum_{n=0}^{k} \left(R_0 + R_d[n]\right) T_s - \frac{d_0}{c} R_0 - m_k \end{aligned} . \tag{13}$$

III. Derivation of equation $\mathbf{B} = \mathbf{HA}$

The impulse response segments are approximated by N-order polynomials:

$$h(\gamma i + i_k', \mu_k') \approx P(\gamma i + i_k', \mu_k') = \sum_{n=0}^{N} b_n(\gamma i + i_k') \mu_k'^{n} , \tag{14}$$

where $P(\gamma i + i_k', \mu_k')$ are N-order polynomials, $b_n(\gamma i + i_k')$ are the polynomial coefficients and are also the coefficients of traditional Farrow structure. We now define the matrix $\mathbf{B}$ of polynomial coefficients as

$$\mathbf{B} = \begin{bmatrix} b_0(-\gamma I) & b_1(-\gamma I) & \cdots & b_N(-\gamma I) \\ b_0(-\gamma I + 1) & b_1(-\gamma I + 1) & & b_N(-\gamma I + 1) \\ \vdots & & \ddots & \vdots \\ b_0(\gamma I - 1) & b_1(\gamma I - 1) & \cdots & b_N(\gamma I - 1) \end{bmatrix} . \tag{15}$$

According to Lagrange interpolation theory, approximating the impulse response segments with N-order polynomials requires $N+1$ basepoints at each segment. For simplicity, we sample each impulse response segment evenly; the sample points must include the segment end points, to ensure continuity of the piecewise polynomial. The sample point coordinates are $\left(nT/N,\ h_n\left(\gamma i+i'_k\right)\right)$, where $h_n\left(\gamma i+i'_k\right)=h\left(\gamma i+i'_k,n/N\right)$, $n=0,\ 1,\ \ldots,\ N$, is the sampled sequence. We now define the sample matrix $\mathbf{H}$ as

$$\mathbf{H}=\begin{bmatrix} h_0\left(-\gamma I\right) & h_1\left(-\gamma I\right) & \cdots & h_N\left(-\gamma I\right) \\ h_0\left(-\gamma I+1\right) & h_1\left(-\gamma I+1\right) & & h_N\left(-\gamma I+1\right) \\ \vdots & & \ddots & \vdots \\ h_0\left(\gamma I-1\right) & h_1\left(\gamma I-1\right) & \cdots & h_N\left(\gamma I-1\right) \end{bmatrix}. \tag{16}$$

Following Lagrange interpolation theory, the *N*-order polynomials $P\left(\gamma i+i'_k,\mu'_k\right)$ can also be written as

$$P\left(\gamma i+i'_k,\mu'_k\right)=\sum_{n=0}^{N}h_n\left(\gamma i+i'_k\right)L_n\left(\mu'_k\right), \tag{17}$$

where $L_n\left(\mu'_k\right)$ is defined as

$$L_n\left(\mu'_k\right)=\prod_{j=0,j\neq n}^{N}\frac{\mu'_kT-\frac{j}{N}T}{\frac{n}{N}T-\frac{j}{N}T}=\sum_{m=0}^{N}a_n\left(m\right)\mu_k'^{m}. \tag{18}$$

The coefficients of polynomial $L_n\left(\mu'_k\right)$ in (18) are defined by matrix $\mathbf{A}$ as

$$\mathbf{A}=\left[a_n\left(m\right)\right]^T, \tag{19}$$

where m is the row index, n is the column index. Table I lists the values of matrix $\mathbf{A}$ when $N=1$, $N=2$, and $N=3$.

We define matrix $\mathbf{L}$ to denote polynomial $L_n\left(\mu'_k\right)$

$$\mathbf{L}=\left[L_0\left(\mu'_k\right)\quad L_1\left(\mu'_k\right)\quad\cdots\quad L_N\left(\mu'_k\right)\right]^T. \tag{20}$$

and define matrix $\mathbf{U}$ to denote the variable of the polynomial.

$$\mathbf{U}=\left[1\quad \mu'_k\quad\cdots\quad \mu_k'^{N}\right]^T. \tag{21}$$

Thus, (18) can be rewritten as

$$\mathbf{L}=\mathbf{AU}. \tag{22}$$

Substituting (17) into (14) yields

$$\mathbf{HL} = \mathbf{BU} . \tag{23}$$

Thus,

$$\mathbf{B} = \mathbf{HA} . \tag{24}$$

Table I Matrix **A** values

Polynomial order	Value
$N=1$	$\begin{bmatrix} 1 & -1 \\ 0 & 1 \end{bmatrix}$
$N=2$	$\begin{bmatrix} 1 & -3 & 2 \\ 0 & 4 & -4 \\ 0 & -1 & 2 \end{bmatrix}$
$N=3$	$\begin{bmatrix} 1 & -\frac{11}{2} & 9 & -\frac{9}{2} \\ 0 & 9 & -\frac{45}{2} & \frac{27}{2} \\ 0 & -\frac{9}{2} & 18 & -\frac{27}{2} \\ 0 & 1 & -\frac{9}{2} & \frac{9}{2} \end{bmatrix}$

IV. Comparison of complexities

The complexities of the Farrow structure and its modifications are listed in Table II.

Table II Complexities of the Farrow structure and its modifications

Structure	Number of multipliers	Number of adders	Number of coefficients
Traditional Farrow structure	$(2I+1)(N+1)-1$	$2I(N+1)-1$	$2I(N+1)$
Modified Farrow structure proposed in [5]	$(I+1)(N+1)$	$2I(N+1)$	$I(N+1)$
Modified Farrow Structure proposed in this paper	$(I+1)(N+1)$	$(2I+1)(N+1)$	$I(N+1)\gamma$

V. Detailed simulation results

We define the PSF as being a raised cosine roll-off filter with a roll-off factor of 0.5; the impulse response of the PSF is truncated with a Hamming window. The detailed properties of the PSFs designed by different methods and parameters are listed in Table III.

Table III Properties of the PSFs designed using different methods and parameters

Method	N	$2I$	γ	δ_p	A_s (dB)	Number of multipliers	Number of adders	Number of coefficients
Lagrange	5	6	1	8.2×10^{-2}	31.5	24	36	18
L_2	5	32	1	7.5×10^{-4}	78.2	102	192	96
Window	5	32	1	2.3×10^{-4}	62.0	102	192	96
Improved Window	5	32	1	1.1×10^{-4}	76.4	102	198	96
Improved Window	5	32	2	1.2×10^{-4}	108.8	102	192	192
Improved Window	5	32	4	1.2×10^{-4}	145.3	102	192	384
Improved Window	5	32	8	1.2×10^{-4}	166.1	102	192	768
Improved Window	4	32	2	1.2×10^{-4}	85.7	85	165	160
Improved Window	3	32	4	1.3×10^{-4}	88.8	68	132	256
Improved Window	2	32	8	1.2×10^{-4}	78.3	51	99	384
Improved Window	1	32	32	1.0×10^{-3}	77.5	34	66	1024

The detailed PSF design and simulation parameters in the comparison of high-dynamic and non-dynamic pulse-shaped signals shown in the Figure 1(e) are listed in Table IV.

Table IV Simulation parameters

Parameters	Value
PSF	Raised-cosine roll-off PSF
Roll-off factor	0.5
f_s	10 MHz
R_0	0.5 Mbps
N	2
$2I$	32
γ	8
Doppler data rate variation model	Cosine function
Doppler data rate variation period	0.1 ms
Maximum Doppler data rate	0.05 Mbps
Initial Doppler data phase	0 rad
Window function	Hamming window